Proceedings of the 2018 IEEE
International Conference on Robotics and Biomimetics
December 12-15, 2018, Kuala Lumpur, Malaysia

Reach-to-Grasp Planning for a Synergy-Controlled Robotic Hand Based on Grasp Quality Prediction*

Zenghui Liu, Zhonghao Wu, Tianlai Dong,
Xiangyang Zhu, *Member, IEEE* and Kai Xu*, *Member, IEEE*

***Abstract*—Grasp analysis of multi-fingered robotic hands has been actively investigated via the use of postural synergies in the past a few years. During grasp planning, the variables for the hand's low-dimensional representation are often optimized together with the hand's position and orientation. The planning optimization terminates when a stable grasp is reached, usually after repetitive trials and resulting in relatively low planning efficiency. This paper proposes a gradient-based algorithm to plan reach-to-grasp task for a robotic hand. The key feature is to predict the grasp quality and adjust the hand's postural synergies, position and orientation in the hand's approaching phase, in order to arrive at a stable grasp with minimal trials. The measure, used for the grasp quality assessment, is modified from the Q distance. The Q distance is a differentiable measure that has been shown highly efficient in quantifying grasp quality. Derivations and formulations of this algorithm are elaborated. The planning for multi-fingered pinches of various objects is successfully realized. Inclusion of additional contact points on the palm would enable the proposed algorithm applicable for grasp planning, eventually leading to a unified framework for efficient reach-to-grasp planning in the near future.**

I. Introduction

Human form various hand poses for grasps and pinches by controlling multiple muscles in a coordinated manner. The coordination is referred to as a postural synergy [1]. The concept of postural synergies (also addressed as EigenGrasps [2]) has triggered lots of research activities from mechanical implementation [3-6] to motion planning and grasp analysis [2, 7-10]. The use of postural synergies is effective due to the fact that a low-dimensional subspace can adequately represent a hand's poses for grasps and pinches as indicated in [11].

When a grasp is planned in this low-dimensional synergy space, the hand's synergy variables are often optimized together with the hand's position and orientation. The optimization terminates when a stable grasp is reached. Various aspects of the grasp planning involving the use of postural synergies have been investigated. For example, a simulated annealing process was used for the grasp optimization in this milestone work by Ciocarlie and Allen [2]. A few representative grasping poses during a search are shown in Fig. 1(a). Other applied searching techniques include the sequential quadratic programming [12], probabilistic roadmap [13], machine learning [14], etc. On the other hand, a low-dimensional representation of the hand's position and orientation was also experimented, in order to reduce the search space. One technique is to use three postural synergies to represent an arm's movements and give the hand's position and orientation via the arm's direct kinematics [13]. Another technique is to extract the postural synergies from hand poses as well as wrist orientations [15].

In the aforementioned grasp planning via the use of the postural synergies, the cost function is usually calculated when the hand is close to the object. The hand's proximity to the object often traps the optimization to a local minimum that represents an unstable grasp, leading to a planning failure. The planning is accomplished usually after repetitive trials and hence resulting in relatively low planning efficiency.

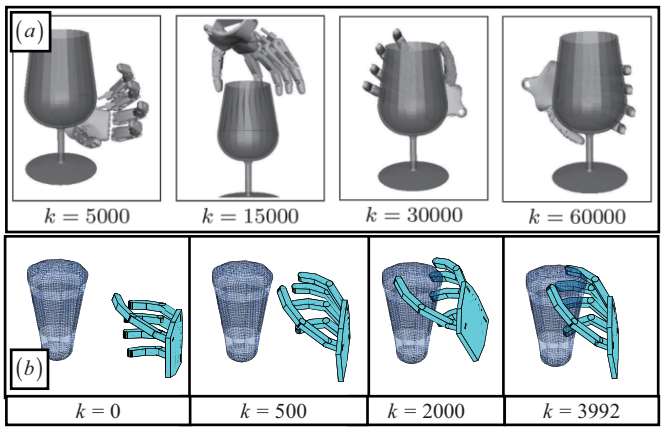

Figure 1. Reach-to-grasp of anthropomorphic hands: (a) hand poses in [2], and (b) hand poses using the presented gradient-based planning

This paper hence proposes to construct a gradient-based algorithm to plan reach-to-grasp tasks for a robotic hand. The key feature is to predict the grasp quality when the hand is still relatively far from the object. The algorithm adjusts the hand's postural synergies, position and orientation when the hand approaches the object, in order to arrive at a stable grasp with minimal trials. A few representative poses of a hand reaching and grasping a cup are shown in Fig. 1(b).

The measure, the scaled Q distance (the sQ distance) that is used for the grasp quality prediction, is modified from the Q distance that was originally proposed by Zhu and Wang [16]. The Q distance is a differentiable measure that has been shown highly efficient in quantifying grasp quality [17].

The main contribution of this work is the proposal and initial validation of this gradient-based algorithm for planning

*This work was supported by the National Natural Science Foundation of China (Grant No. 51435010, Grant No. 51722507 and Grant No. 91648103).

Zenghui Liu, Zhonghao Wu and Tianlai Dong are with the RII Lab (Lab of Robotics Innovation and Intervention), UM-SJTU Joint Institute, Shanghai Jiao Tong University, Shanghai, China (emails: liuzenghui@sjtu.edu.cn, zhonghao.wu@sjtu.edu.cn, and 5123709073@sjtu.edu.cn).

Xiangyang Zhu and Kai Xu are with the School of Mechanical Engineering, Shanghai Jiao Tong University, Shanghai, China (emails: mexyzhu@sjtu.edu.cn and k.xu@sjtu.edu.cn, corresponding author: K. Xu).

978-1-7281-0377-8/18/$31.00 © 2018 IEEE

a hand's reach-to-grasp tasks. Multi-fingered pinch planning of various objects has been successfully realized. Inclusion of additional contact points on the palm would enable the proposed algorithm applicable for power grasp planning. The effectiveness essentially lies on two aspects: i) the sQ distance can predict the grasp quality; ii) the differentiability of the sQ distance enables the implementation.

The paper is organized as follows. Section II presents a derivation summary of the Q distance, while Section III presents the description of the synergy-based hand as well as the formulation of the reach-to-grasp planning algorithm. The computational experiments are reported in Section IV with discussions and future works summarized in Section V.

II. A Summary of the Q Distance

The Q distance was originally proposed for efficient grasp planning [16]. Relevant conclusions are summarized here for readers' convenience.

As shown in Fig. 2, an object is grasped with n contact points with Coulomb friction. The hard finger contact model with friction from [18] is used. The friction cone $C(\mathbf{p}_i)$ is linearized by an m-sided polyhedral cone. The cone's edge vectors $\mathbf{d}_1(\mathbf{p}_i)$, ⋯, $\mathbf{d}_m(\mathbf{p}_i)$, satisfying the constraint in (1).

$$\mathbf{d}_j(\mathbf{p}_i)\cdot\mathbf{n}_i = 1,\ i = 1, 2, \cdots, n \text{ and } j = 1, 2, \cdots, m \tag{1}$$

Where $\mathbf{n}_i$ is a unit normal vector of the surface at the contact point $\mathbf{p}_i$, pointing towards inside the object.

Any contact force $\mathbf{f}_i$ at the contact point $\mathbf{p}_i$ can hence be expressed as in (2). Sum of the non-negative coefficients α_{ij} describes the amplitude of the normal component of the contact force $\mathbf{f}_i$ as in (3). The contact wrench $\mathbf{w}_i$ produced by the contact force $\mathbf{f}_i$ is written in (4).

$$\mathbf{f}_i = \sum_{j=1}^{m} \alpha_{ij}\mathbf{d}_j(\mathbf{p}_i) \tag{2}$$

$$\mathbf{f}_i\cdot\mathbf{n}_i = \sum_{j=1}^{m} \alpha_{ij}\mathbf{d}_j(\mathbf{p}_i)\cdot\mathbf{n}_i = \sum_{j=1}^{m}\alpha_{ij} \tag{3}$$

$$\mathbf{w}_i = \begin{bmatrix}\mathbf{f}_i \\ \mathbf{p}_i\times\mathbf{f}_i\end{bmatrix} = \sum_{j=1}^{m}\alpha_{ij}\mathbf{w}_{ij} \text{ and } \mathbf{w}_{ij} = \begin{bmatrix}\mathbf{d}_j(\mathbf{p}_i) \\ \mathbf{p}_i\times\mathbf{d}_j(\mathbf{p}_i)\end{bmatrix} \tag{4}$$

The grasp quality is evaluated by a Q distance (Q^+ or Q^-).

The Q^+ distance shall be calculated first as a linear programming problem as in (5).

$$d_Q^+(\mathbf{u}) = \min \sum_{k=1}^{K}\rho_k$$
$$s.t.\begin{cases}\sum_{i=1}^{n}\sum_{j=1}^{m}\alpha_{ij} = 1,\ \alpha_{ij}\ge 0 \\ \sum_{k=1}^{K}\rho_k\mathbf{q}_k = \sum_{i=1}^{n}\sum_{j=1}^{m}\alpha_{ij}\mathbf{w}_{ij},\ \rho_k\ge 0\end{cases} \tag{5}$$

Where the grasp configuration $\mathbf{u}$ determines the contact points $\mathbf{p}_i$; the contact points $\mathbf{p}_i$ give the elementary wrench $\mathbf{w}_{ij}$ from (4); $\mathbf{q}_k$ are the vertices of a simplex. The minimal dimension of the simplex is 6 as adopted from [16]. The number of the vertices K is 7 and ρ_k is the coefficient for the vertices $\mathbf{q}_k$.

If the Q^+ distance is calculated as zero (or less than 10^{-3} in the actual implementation), the Q^- distance shall be calculated as a second linear programming problem in (6) and (7).

$$d_Q^-(\mathbf{u}) = \max_{k=1,\ldots,K} d_Q^-(k) \tag{6}$$

$$d_Q^-(k) = \min(-\rho)$$
$$s.t.\begin{cases}\sum_{i=1}^{n}\sum_{j=1}^{m}\alpha_{ij} = 1,\ \alpha_{ij}\ge 0 \\ \rho\mathbf{q}_k = \sum_{i=1}^{n}\sum_{j=1}^{m}\alpha_{ij}\mathbf{w}_{ij},\ \rho\ge 0\end{cases} \tag{7}$$

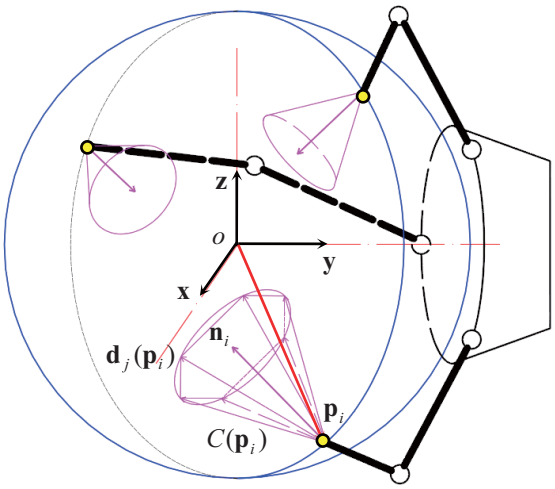

Figure 2. Frictional point contacts on an object

Shown in [16], the Q distance (Q^+ or Q^-) is differentiable. The differentiability directly enables this gradient-based reach-to-grasp algorithm. The derivatives of the Q^+ or Q^- distances w.r.t the grasp configuration $\mathbf{u}$, are available in [16].

III. Descriptions of the Synergy-Based Hand and Formulation of the Grasp Planning Algorithm

Description of the synergy-based hand is presented in Section III.A, while formulation of the gradient-based grasp planning algorithm is presented in Section III.B.

A. Synergy-Based Hand

The synergy-based hand has 11 joints: three for the thumb and two for each finger. The *T*, *I*, *M*, *R* and *L* letters indicate the thumb, the index, the middle, the ring and the little fingers. Abbreviations of *rot*, *mcp*, *ip*, *abd*, *pip* and *dip* indicate the rotation, the metacarpophalangeal, the interphalangeal, the abduction, the proximal and the distal interphalangeal joints respectively. The T_{ip} joint and the *dip* joints of the fingers are fixed to 20° to simplify the hand structure. In addition, the *pip*

joints are coupled to the *mcp* joints of the fingers and the T_{mcp} joint is coupled to the T_{abd} joint with a ratio of 1:1 for simplification. The synergy-based hand is shown in Fig. 3.

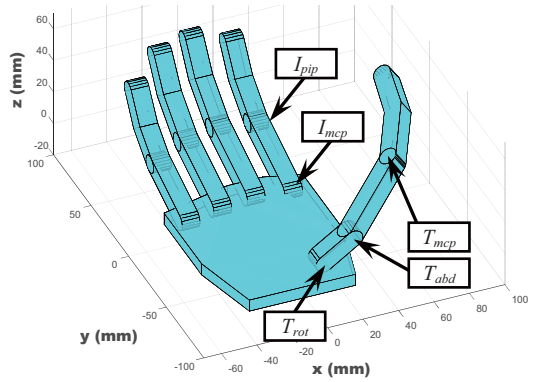

Figure 3. Structure and joint assignments of the synergy-based hand

The phalange lengths were firstly set according to a study on hand anatomy [19]. However, directly using the original statistical values of the phalange lengths in [19] leads to the result that the middle finger is about 10 mm longer than the index finger. Although this might be true for actual human anatomy, this length difference can negatively impact the stability of the planned grasps. Then the intermediate and proximal phalange lengths were modified according to [20]. All the phalange lengths, which are rounded to millimeters, are listed in Table I.

TABLE I. STRUCTURAL PARAMETERS OF THE SIMULATED HAND

	Thumb	Index	Middle	Ring	Little
Distal phalange	27 mm	20 mm	21 mm	21 mm	20 mm
Intermediate phalange	-	25 mm	28 mm	27 mm	21 mm
Proximal phalange	32 mm	47 mm	48 mm	46 mm	40 mm
Metacarpal	46 mm	-	-	-	-

Since the synergy-based hand has six independently actuated joints (the T_{rot}, T_{abd}, I_{mcp}, M_{mcp}, R_{mcp} and L_{mcp} joints), the hand pose is represented as a six dimensional pose vector $\boldsymbol{\psi}$. Then the postural synergies of the hand can be extracted from a group of grasping and pinching poses. The poses from a previous study in [5] are used, where the anthropomorphic hand grasped a dozen of daily-life objects including a tennis ball, a book, a cup, a pill jar, a box, a tape roll, a can, a screw driver, a bottle and a mug. Then the extracted postural synergies ($\mathbf{s}_1$ and $\mathbf{s}_2$) and the average pose $\bar{\boldsymbol{\psi}}$ are reported in Table II. A hand pose can be approximated as in (8).

$$\boldsymbol{\psi} = \bar{\boldsymbol{\psi}} + [\mathbf{s}_1 \quad \mathbf{s}_2][z_1 \quad z_2]^T \tag{8}$$

Where z_1 and z_2 are the synergy variables. Elements of the postural synergies $\mathbf{s}_1$ and $\mathbf{s}_2$ are listed as the matching cells in Table II.

Changing the synergy variables of z_1 and z_2 would change the hand poses. The hand poses are shown in Fig. 4 while changing z_1 and z_2 between [-1, 1].

TABLE II. THE EXTRACTED POSTURAL SYNERGIES (UNIT: RAD)

	T_{rot}	T_{abd}	I_{mcp}	M_{mcp}	R_{mcp}	L_{mcp}
Synergy1	-0.2137	0.0490	0.0676	0.2573	0.2991	0.3279
Synergy2	-0.1731	-0.1318	-0.3853	-0.4756	-0.4316	-0.3440
$\bar{\boldsymbol{\psi}}$	1.2140	0.4030	0.6616	0.7145	0.7723	0.8875

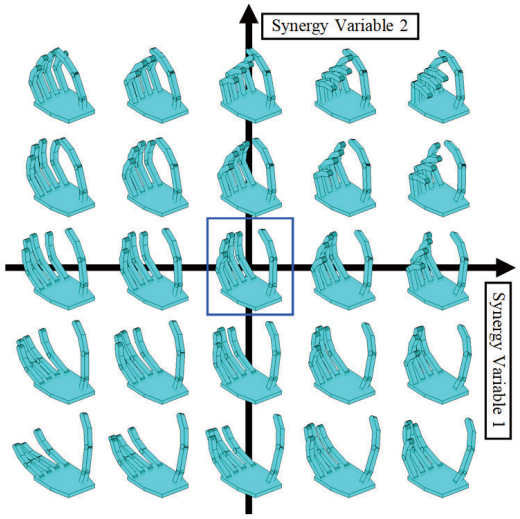

Figure 4. Hand poses under different synergy variables on the synergy plane with the average pose shown inside the central blue box

B. Gradient-Based Grasp Planning

The grasp configuration $\mathbf{u} = [p_x\ p_y\ p_z\ \phi_1\ \phi_2\ \phi_3\ z_1\ z_2]^T$ includes the synergy variables (z_1 and z_2) and the position (p_x, p_y and p_z) and the orientation (three Euler angles: ϕ_1, ϕ_2 and ϕ_3, the XYZ yaw-pitch-roll representation) of the palm. Even though the Euler angles may be subject to possible singularity, it is considered a less important issue in this problem because the palm's orientation is not expected to change dramatically.

Goal of the proposed algorithm is to adjust the hand's postural synergy variables, the palm's position and orientation while the hand approaches an object, in order to arrive at a stable grasp with minimal trials. This requires the proposed algorithm to predict the grasp quality when the hand is relatively far from the object.

Based on the Q distance in [16], this paper proposes a scaled Q distance (the sQ distance) for predicting the grasp quality. As illustrated by Fig. 5, the to-be-grasped object is positioned away from the hand, touching none of the fingers. Then the object is proportionally scaled such that the scaled object would get in touch with the tip of each finger including the thumb. The hand's five fingers would correspond to five scale factors: g_T, g_I, g_M, g_R and g_L. Using the five contact points between the fingers and the scaled objects, the sQ distance (g_{sQ}) can be calculated from (5) and (6). Then a status vector $\mathbf{g}$ for the reach-to-grasp task can be defined as follows.

$$\mathbf{g} = \begin{bmatrix} g_T & g_I & g_M & g_R & g_L & g_{sQ} \end{bmatrix}^T \tag{9}$$

In the implementation, the scaled factor for a finger was calculated as the ratio of the distance from the object center to a point on the object surface that is closest to the fingertip over

the distance from the object center to the fingertip. This was designed to increase the numerical stability when the object to be grasped has a local concave feature.

When the scale factors (g_T, g_I, g_M, g_R and g_L) approach ones, the hand's fingers are touching the surface of the object to be grasped. Then when $g_{sQ} < 0$, a stable grasp is achieved. It is of course possible that only three or four out of the five fingers touches the object's surface at the same time, since these fingers are not independently actuated. Detailed handling would be explained later in this section.

Currently, only multi-fingered pinches (a.k.a. precision grasp) are planned in this paper, since the status vector **g** only includes the scale factors concerning the tip of the five fingers. The algorithm can be easily extend to power grasp planning if additional contact points are allocated on the palm.

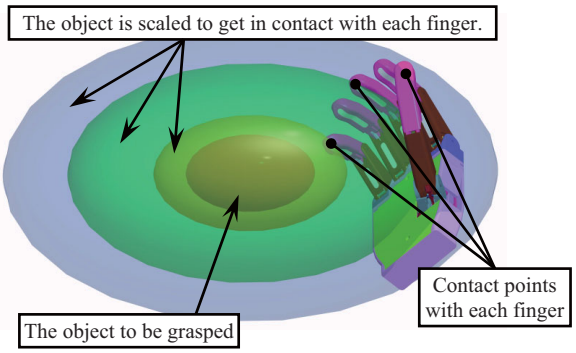

Figure 5. The scaled to-be-grasped object leading to the sQ distance

The status vector **g** depends on the grasp configuration **u**. Then a Jacobian matrix $\mathbf{J}_g$ can be derived, using the derivative of the Q distance from [19].

$$\mathbf{J}_g = \left[\frac{\partial \mathbf{g}}{\partial u_1} \quad \cdots \quad \frac{\partial \mathbf{g}}{\partial u_8} \right] = \begin{bmatrix} \frac{\partial g_1}{\partial u_1} & \cdots & \frac{\partial g_1}{\partial u_8} \\ \vdots & \ddots & \vdots \\ \frac{\partial g_6}{\partial u_1} & \cdots & \frac{\partial g_6}{\partial u_8} \end{bmatrix} \tag{10}$$

An iterative gradient-based algorithm for planning the reach-to-grasp tasks can be constructed as in Fig. 6. The iterations start with the target grasp status vector $\mathbf{g}^t$ and the current grasp status vector $\mathbf{g}^c$. Then the difference between the target and the current values of the grasp status vector $\boldsymbol{\varepsilon} = \mathbf{g}^t - \mathbf{g}^c$ is obtained. If the difference $\boldsymbol{\varepsilon}$ satisfies the stop criterion as stated below, the iterations will terminate and the planning is finished. Otherwise, desired increment of the status vector $\Delta\mathbf{g}$ is obtained as in (11). Then the desired increment of the grasp configuration $\Delta\mathbf{u}$ is obtained as in (12), where the Jacobian $\mathbf{J}_g$ is from (10). In possible cases of singularity, a singularity robust formulation of $\mathbf{J}_g^+$ is used. The grasp configuration **u** is updated as $\mathbf{u} = \mathbf{u} + \Delta\mathbf{u}$. Using the updated grasp configuration **u**, the fingertip positions are obtained and the new grasp status vector **g** can be obtained. This would start a new iteration.

$$\Delta\mathbf{g} = \mathbf{V}\boldsymbol{\varepsilon} \tag{11}$$

Where $\mathbf{V} = \mathrm{diag}(v_1, v_2, \cdots, v_6)$ is a control matrix that adjusts the convergence speed.

$$\Delta\mathbf{u} = \mathbf{J}_g^+ \Delta\mathbf{g} \tag{12}$$

The stop criterion is satisfied for the following condition. When the scale factors for the thumb and two or three of the other four fingers are within the range from 0.98 to 1.02, the Q distance calculated from the three or four corresponding tip points of the contacting fingers is less than -0.1. The calculation of the Q distance here excludes the non-contacting finger(s). Hence it is a Q distance, instead of a sQ distance. A Q distance value of -0.1 to -0.2 is typical from the previous investigation in [19].

The maximal number of the iterations is set to 10000. When this number is reached, the iterative grasp planning is terminated. The planning can still be considered successful if three or more fingers are touching the object surface and the Q distance calculated from the contacting fingertips is negative. The grasp is a force-closure one, as long as the calculated Q distance value is negative.

When the maximal number of iterations is reached, the planned grasp fails if only two fingers touch the object surface, or three or more fingers are touching with a positive Q distance calculated from the contacting fingertips. The constructed algorithm is inspired by the resolved rates algorithm for Jacobian-based manipulator control in [21].

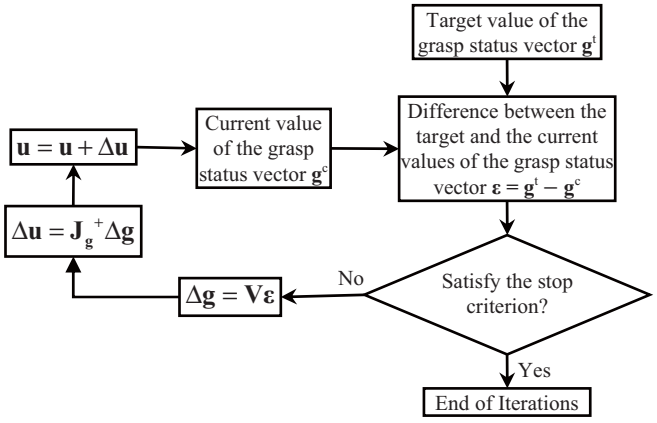

Figure 6. Flow chart of the gradient-based grasp planning algorithm

IV. Computational Experiments

In order to initially demonstrate the effectiveness of the proposed algorithm, a series of computational experiments were carried out. The reach-to-grasp tasks for a cylinder and a curved object are presented.

During these computational experiments, the friction coefficient between the object and the fingers is set at 0.3. The friction cone is linearized by an eight-sided polyhedral cone ($m = 8$). The target grasp status vector $\mathbf{g}^t$ is set as $[1\ 1\ 1\ 1\ 1\ -1]^T$. The first five ones in $\mathbf{g}^t$ drive the fingers to touch the object surface, while the last constant of -1 drives the hand to form a stable pose.

A. Reach to Grasp a Cylinder

The proposed gradient-based iterative grasp planning algorithm was firstly tested on a cylinder. Differentiability of the Q distance is only guaranteed when the surfaces touched by the fingers are locally smooth [19]. Hence the intended surface for the grasp is the cylindrical lateral one, as in Fig. 7. The cylinder has a diameter of 60 mm and a height of 200 mm. Its center is located at the origin of the reference frame.

The fingertip points can be calculated from the grasp configuration **u** that includes the synergy variables, the hand's position and orientation. The scale factors of the five fingers (g_T, g_I, g_M, g_R and g_L) were calculated according to Section III.B. Using the positions of the fingertips while the hand approaches the cylinder, the sQ distance (the g_{sQ} value) can be calculated from (5) to (7).

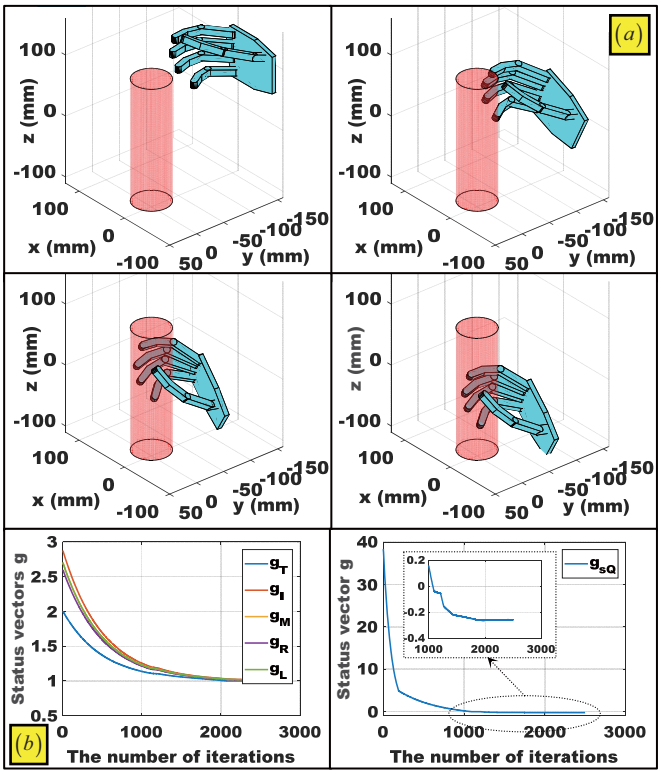

Figure 7. Reach to grasp a cylinder: (a) hand poses, and (b) status vector g

In the implemented algorithm, the control matrix **V** that adjusts the convergence speed is set as in (13).

$$\mathbf{V} = \begin{cases} \mathrm{diag}(1,1,1,1,1,5)\times 10^{-3}, & g_{sQ} \geq 5 \\ \mathrm{diag}(1,1,1,1,1,1)\times 10^{-3}, & g_{sQ} < 5 \end{cases} \quad (13)$$

Where the coefficient of 10^{-3} is necessary for generating smoothly changing hand poses.

The hand poses and the values of the grasp status vector **g** for the reach-to-grasp motion of the cylinder are shown in Fig. 7 as well as in the multimedia extension.

At the beginning of the reach-to-grasp process, the hand in its average pose is placed away from the cylinder to be grasped. The sQ distance (the g_{sQ} value) is 38.39, predicting a highly unstable grasp. Under this proposed algorithm, the hand firstly opens its fingers while approaching the cylinder, and then closes its fingers to achieve a stable grasp.

When $g_{sQ} \geq 5$, the values in the control matrix **V** lead to a rapid drop in g_{SQ}. After 190 iterations, g_{sQ} reached below 5 and the new values in **V** produced a slower drop in g_{SQ}.

Since the sQ distance (as well as the Q distance) is calculated with respect to the center of the cylinder, the hand tried to grasp the cylinder around the center.

The iterations stopped at the index of 2304 and the total simulation time in MATLAB 2015 was 490 seconds on a laptop with an Intel i5-2430M CPU and 4 GB memory. The terminating scale factors of the five fingers (g_T, g_I, g_M, g_R and g_L) are 0.999, 1.020, 1.014, 1.013 and 1.016 respectively with the Q distance of -0.259. On the iteration at index of 2303, the scale factors are 0.9999, 1.0201, 1.0143, 1.0131 and 1.0163 respectively. The index finger is considered not touching the cylinder since the scale factor (1.0201) is larger than 1.02. Under that pose, the Q distance was calculated as 0.172 excluding the non-touching index finger, which does not satisfy the terminating criterion. Then the iteration goes on to the index of 2304. The scale factor of the index finger satisfies the contacting condition. Hence a negative Q distance value was obtained, counting on the index finger. Please note that the plot in Fig. 7(b) is for the sQ values, which includes all the fingertips and is hence without sudden jumps.

B. Reach to Grasp a Curved Object

Then the proposed algorithm was tested on a curved object with concave surfaces to demonstrate the robustness of the algorithm. The object's shape was generated by revolving a curve for 360°. Other settings are identical to those for the cylinder. The hand poses and the values of the grasp status vector **g** for the reach-to-grasp motion are shown in Fig. 8 and in the multimedia extension.

It can be seen from Fig. 8 that the scaled factor for the ring finger (g_R) fluctuated during the approaching phase, since this finger was pointing towards the object's concave "waist". But this fluctuation does not impact the algorithm's overall trend. The g_{sQ} value in Fig. 8(b) still monotonically decreased. When the iterations were terminated, the scale factors of the five fingers (g_T, g_I, g_M, g_R and g_L) are 0.9978, 1.0074, 1.0190, 1.0021 and 1.0062 respectively with the Q distance at -0.1383. The total simulation time on the same laptop is 747 seconds.

Cylinders with different diameters and other objects (e.g., the cup in Fig. 1) were also tested. Similar results were obtained.

V. Discussions and Future Work

This paper proposes a gradient-based iterative algorithm for reach-to-grasp planning on a synergy hand, via grasp quality prediction, aiming at adjusting the pose, the position and the orientation of a hand when it approaches the object to be grasped, achieving a stable grasp with minimal attempts.

Through a series of computational experiments, efficacy of the algorithm is initially validated. The results look promising even though there are abundant amount of future work can be carried out immediately.

The first work item is to include several contact points on the palm so that power grasps can also be planned. Then an adaptive policy for updating the control matrix **V** during the iterations can be designed such that a stable grasp can be achieved more quickly. Last but not the least, the grasp configuration **u** has eight elements, while the grasp status vector **g** contains six. A weight matrix can be included into the proposed iterative algorithm to limit rotations of the palm. Currently the hand often adjusts the wrist's twist (hand supination/pronation about the forearm) for (slightly) better grasp quality. This minor gain makes the hand pose unnatural and should be limited. It is expected that the proposed algorithm could be developed into a unified framework for efficient planning of reach-to-grasp tasks in the near future.

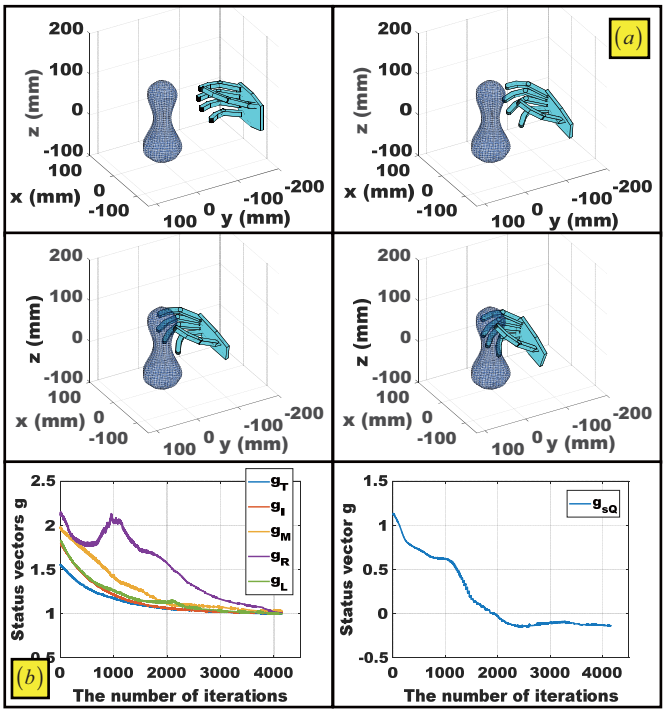

Figure 8. Reach to grasp a curved object: (a) hand poses, and (b) status vector

REFERENCES

[1] N. Bernstein, "The Problem of the Interrelation of Coordination and Localization," *Archives of Biological Sciences,* vol. 38, No.1, pp. 1-34, 1935.

[2] M. T. Ciocarlie and P. K. Allen, "Hand Posture Subspaces for Dexterous Robotic Grasping," *The International Journal of Robotics Research,* vol. 28, No.7, pp. 851-867, June 2009.

[3] C. Y. Brown and H. H. Asada, "Inter-Finger Coordination and Postural Synergies in Robot Hands via Mechanical Implementation of Principal Components Analysis," in *IEEE/RSJ International Conference on Intelligent Robots and Systems (IROS)*, San Diego, CA, USA, 2007, pp. 2877-2882.

[4] K. Xu, H. Liu, Y. Du, and X. Zhu, "Design of an Underactuated Anthropomorphic Hand with Mechanically Implemented Postural Synergies," *Advanced Robotics,* vol. 28, No.21, pp. 1459-1474, Nov 2014.

[5] K. Xu, H. Liu, Y. Du, X. Sheng, and X. Zhu, "Mechanical Implementation of Postural Synergies Using a Simple Continuum Mechanism," in *IEEE International Conference on Robotics and Automation (ICRA)*, Hong Kong, China, 2014, pp. 1348-1353.

[6] W. Chen, C. Xiong, and S. Yue, "Mechanical Implementation of Kinematic Synergy for Continual Grasping Generation of Anthropomorphic Hand," *IEEE/ASME Transactions on Mechatronics,* vol. 20, No.3, pp. 1249-1263, May 2015.

[7] G. C. Matrone, C. Cipriani, E. L. Secco, M. C. Carrozza, and G. Magenes, "Bio-Inspired Controller for a Dexterous Prosthetic Hand Based on Principal Components Analysis," in *Annual International Conference of the IEEE Engineering in Medicine and Biology Society (EMBS)*, Minneapolis, Minnesota, USA, 2009, pp. 5022-5025.

[8] A. Bicchi, M. Gabiccini, and M. Santello, "Modelling Natural and Artificial Hands with Synergies," *Philosophical Transactions of the Royal Society B: Biological Sciences,* vol. 366, No.1581, pp. 3153-3161, Nov 2011.

[9] M. Gabiccini, E. Farnioli, and A. Bicchi, "Grasp Analysis Tools for Synergistic Underactuated Robotic Hands," *International Journal of Robotics Research,* vol. 32, No.13, pp. 1553-1576, Nov 2013.

[10] G. Palli, C. Melchiorri, G. Vassura, U. Scarcia, L. Moriello, G. Berselli, A. Cavallo, G. D. Maria, C. Natale, S. Pirozzi, C. May, F. Ficuciello, and B. Siciliano, "The DEXMART Hand: Mechatronic Design and Experimental Evaluation of Synergy-Based Control for Human-Like Grasping," *International Journal of Robotics Research,* vol. 33, No.5, pp. 799-824, April 2014.

[11] M. Santello, M. Flanders, and J. F. Soechting, "Postural Hand Synergies for Tool Use," *The Journal of Neuroscience,* vol. 18, No.23, pp. 10105-10115, Dec 1998.

[12] C. I. Mavrogiannis, C. P. Bechlioulis, M. V. Liarokapis, and K. J. Kyriakopoulos, "Task-Specific Grasp Selection for Underactuated Hands," in *IEEE International Conference on Robotics and Automation (ICRA)*, Hong Kong, China, 2014, pp. 3676-3681.

[13] J. Rosell, R. Suárez, C. Rosales, and A. Pérez, "Autonomous Motion Planning of a Hand-Arm Robotic System Based on Captured Human-like Hand Postures," *Autonomous Robots,* vol. 31, No.1, pp. 87-102, 2011.

[14] H. B. Amor, O. Kroemer, U. Hillenbrand, G. Neumann, and J. Peters, "Generalization of Human Grasping for Multi-Fingered Robot Hands," in *IEEE/RSJ International Conference on Intelligent Robots and Systems (IROS)*, Vilamoura, Algarve, Portugal, 2012, pp. 2043-2050.

[15] A. Provenzale, F. Cordella, L. Zollo, A. Davalli, R. Sacchetti, and E. Guglielmelli, "A Grasp Synthesis Algorithm Based on Postural Synergies for an Anthropomorphic Arm-Hand Robotic System," in *IEEE / RAS-EMBS International Conference on Biomedical Robotics and Biomechatronics (BIOROB)*, São Paulo, Brazil, 2014, pp. 958-963.

[16] X. Zhu and J. Wang, "Synthesis of Force-Closure Grasps on 3-D Objects Based on the Q Distance," *IEEE Transactions on Robotics and Automation,* vol. 19, No.4, pp. 669-679, Aug 2003.

[17] N. S. Pollard, "Closure and Quality Equivalence for Efficient Synthesis of Grasps from Examples," *The International Journal of Robotics Research,* vol. 23, No.6, pp. 595-613, June 2004.

[18] R. M. Murray, Z. Li, and S. S. Sastry, *A Mathematical Introduction to Robotic Manipulation*: CRC Press, 1994.

[19] B. Alexander and K. Viktor, "Proportions of Hand Segments," *International Journal of Morphology,* vol. 28, No.3, pp. 755-758, 2010.

[20] R. Hamilton and R. A. Dunsmuir, "Radiographic Assessment of the Relative Lengths of the Bones of the Fingers of the Human Hand," *Journal of Hand Surgery (British and European Volume),* vol. 27, No.6, pp. 546-548, 2002.

[21] D. E. Whitney, "Resolved Motion Rate Control of Manipulators and Human Prostheses," *IEEE Transactions on Man-Machine Systems,* vol. 10, No.2, pp. 47-53, June 1969.